The Bioscan AN INTERNATIONAL QUARTERLY JOURNAL OF LIFE SCIENCES 20(4): 2074-2093, 2025 www.thebioscan.com

Formulation Development and Pharmacological Evaluation of Curcumin–Resveratrol Co-Loaded Lipid Nanoparticles for Synergistic Protection Against Diabetic Cardiomyopathy in Type 2 Diabetes Mellitus

A. Seetha Devi*
Professor, Department of Pharmaceutics, Gokaraju Rangaraju College of Pharmacy, Bachupally, Hyderabad, Telangana 500090, India. Email: seethagottipati@gmail.com

DOI: 10.63001/tbs.2025.v20.i04.pp2074-2093

Keywords

Co-delivery; Diabetic cardiomyopathy; Lipid nanoparticles; Nanomedicine; Oxidative stress.

Received on:

22-10-2025

Accepted on:

17-11-2025

Published on:

31-12-2025

ABSTRACT

The study focused on the development and evaluation of curcumin–resveratrol co-loaded lipid nanoparticles (CL-LNPs) as a synergistic therapeutic platform for type 2 diabetes–associated cardiomyopathy. The nanoparticles were fabricated using a modified hot-emulsion ultrasonication method and characterized for particle size, polydispersity index, zeta potential, entrapment efficiency, and release behaviour. The optimized CL-LNPs exhibited uniform nanoscale dimensions, low PDI values, and a sufficiently negative zeta potential, indicating excellent colloidal stability. Both curcumin and resveratrol achieved high entrapment within the lipid matrix, and the system demonstrated a sustained-release profile extending up to 48 hours. Antioxidant analyses, including DPPH, ABTS, and nitric oxide assays, revealed markedly enhanced radical-scavenging activity for the co-loaded nanoparticles compared with free curcumin, free resveratrol, and single-drug-loaded formulations. Anti-inflammatory evaluations similarly showed superior inhibition of protein denaturation and improved stabilization of human RBC membranes, confirming enhanced modulation of inflammatory pathways. Cytotoxicity studies on H9c2 cardiomyocytes demonstrated improved cell viability and significantly lower IC_{50} values for the co-loaded system. Additionally, intracellular ROS quantification and LDH leakage assays confirmed strong cytoprotective and membrane-stabilizing effects, indicating effective attenuation of oxidative and metabolic injury. Overall, the results suggest that curcumin–resveratrol co-loaded lipid nanoparticles offer a highly promising strategy for targeting oxidative stress, inflammation, and cellular damage in diabetic cardiomyopathy. Their synergistic dual-drug efficacy underscores strong potential for further in-vivo exploration and future translational application in diabetes-associated cardiovascular disorders.

INTRODUCTION

Type 2 diabetes mellitus (T2DM) is a widespread metabolic disorder that leads to severe long-term complications, including diabetic cardiomyopathy—now recognised as a major cardiac consequence of diabetes. This condition involves structural and functional myocardial damage occurring independently of hypertension or coronary artery disease. Chronic hyperglycaemia triggers oxidative stress, inflammation, mitochondrial dysfunction, and accumulation of advanced glycation end products, collectively promoting myocardial remodelling, fibrosis, and gradual cardiac failure. These interconnected mechanisms limit the effectiveness of conventional therapies. Standard antidiabetic drugs and antioxidants offer only modest improvement due to poor solubility, rapid degradation, low tissue permeability, and insufficient cardiac targeting. This highlights the need for advanced therapeutic strategies capable of simultaneously modulating multiple pathological pathways (Abdelsaid *et al.*, 2016; Cryer *et al.*, 2016; Karam *et al.*, 2017; Wong *et al.*, 2017).

Lipid-based nanocarriers have recently emerged as promising systems for enhancing drug delivery in metabolic and cardiovascular disorders. Their biocompatibility, biodegradability, and resemblance to natural membranes allow them to efficiently encapsulate therapeutic molecules, improve drug stability, enable controlled release, and promote better cellular uptake. These advantages are especially valuable for drugs with poor solubility or limited bioavailability in traditional formulations. Importantly, the ability to co-encapsulate multiple agents within one nanocarrier supports synergistic therapeutic effects, lowers dosing frequency, and allows simultaneous targeting of several pathological pathways. This approach is particularly suited for diabetic cardiomyopathy, where oxidative stress, inflammation, and cellular injury collectively drive disease progression (Abdelsaid *et al.*, 2016; Bathina & Das, 2018; Bogdanov *et al.*, 2018; Ighodaro *et al.*, 2017; Nakhate *et al.*, 2016).

Combining antioxidant and anti-inflammatory agents has been identified as an effective strategy for reducing myocardial dysfunction in T2DM. However, free drugs often suffer from rapid clearance, poor pharmacokinetics, and limited cardiac accumulation. Nanocarrier-based co-delivery systems address these limitations by improving solubility, extending circulation time, protecting drugs from degradation, and supporting sustained release. Lipid nanoparticles are especially well suited for encapsulating lipophilic or moderately lipophilic molecules, ensuring efficient loading and improved intracellular retention. By maintaining therapeutic levels for longer durations, these nanoparticles offer a promising means to counteract the oxidative and inflammatory damage central to diabetic cardiomyopathy (Alwafi *et al.*, 2020; Andrade *et al.*, 2020; Arroyave *et al.*, 2020; Arvanitakis *et al.*, 2020; Avilés-Santa *et al.*, 2020; Wong *et al.*, 2017).

Although nanomedicine has gained momentum in treating metabolic and cardiovascular diseases, research on co-loaded lipid nanoparticles for diabetic cardiomyopathy remains scarce. Most existing work focuses on single-drug systems or non-lipid carriers, leaving a clear gap regarding dual-drug lipid nanocarriers tailored for cardiac protection. Developing co-loaded nanoparticles that deliver complementary therapeutic agents offers a promising strategy to enhance cardioprotection, limit oxidative injury, and stabilize myocardial function in T2DM. Based on this need, the present study aimed to design and evaluate curcumin–resveratrol co-loaded lipid nanoparticles for synergistic management of diabetic cardiomyopathy. The formulation was prepared using a modified hot-emulsion ultrasonication method and subjected to thorough physicochemical and in-vitro biological characterization. Key parameters assessed included particle size, PDI, zeta potential, entrapment efficiency, drug release kinetics, antioxidant capacity, anti-inflammatory activity, cytotoxicity, intracellular ROS reduction, and membrane-protective effects. By integrating two therapeutic agents (Curcumin and Resveratrol) within a single lipidic carrier, the study sought to create a stable, sustained-release nanomedicine capable of targeting the multiple pathological pathways involved in diabetic cardiomyopathy. The outcomes of this work provide a strong basis for future in-vivo studies and potential clinical advancement of the co-loaded lipid nanoparticle system as an innovative therapeutic option for diabetes-related cardiac complications.

MATERIALS AND METHODS

Materials

Phosphatidylcholine (PC), cholesterol, glyceryl monostearate (GMS), and medium-chain triglycerides (MCT oil) used in the formulation work were sourced from HiMedia Laboratories, Mumbai, India. The surfactants and co-surfactants, including Tween-80, Poloxamer-188, and PEG-400, were purchased from Sigma-Aldrich, USA. Curcumin, selected for its potent antioxidant and anti-inflammatory potential, and

resveratrol, recognised for its antidiabetic and cardioprotective activity, were obtained as gift samples from a reputed pharmaceutical manufacturer. High-performance liquid chromatography (HPLC)-grade solvents such as methanol, ethanol, acetonitrile, and chloroform were procured from Merck, Darmstadt, Germany, to ensure analytical precision. Materials required for the in-vitro evaluation—DPPH and ABTS free-radical scavenging reagents, Griess reagent, MTT and LDH assay kits, the DCFH-DA probe for intracellular ROS assessment, and ELISA kits for cytokine quantification—were supplied by Sigma-Aldrich and Abcam. All chemicals and reagents used throughout the study adhered to analytical-grade standards, ensuring reliability and reproducibility of experimental outcomes.

Preparation of Co-Loaded Lipid Nanoparticles (CL-LNPs)

Co-loaded lipid nanoparticles containing curcumin and resveratrol were prepared using a modified hot-emulsion ultrasonication method. Initially, the lipid components comprising phosphatidylcholine (PC), cholesterol, and glyceryl monostearate (GMS) were heated to 75–80°C to obtain a uniform lipid melt. Curcumin and resveratrol were separately dissolved in a small volume of warm ethanol and introduced gradually into the molten lipid phase with constant stirring to ensure complete molecular dispersion. A hot aqueous phase containing Tween-80 and Poloxamer-188, maintained at the same temperature, was then added slowly to the lipid phase under high-speed stirring (8000 rpm), resulting in the formation of a coarse oil-in-water emulsion. This emulsion was subsequently subjected to probe ultrasonication at 40% amplitude with intermittent pulses for 5–8 minutes to reduce the droplet size and achieve nanoscale dispersion. The nanoemulsion was rapidly cooled in an ice bath to solidify the lipid droplets and form stable nanoparticles. The final dispersions were transferred to amber vials and stored at 4°C until further use. Blank nanoparticles and single-drug-loaded nanoparticles were prepared following the same procedure (Ahangarpour *et al.*, 2018; Aldayel *et al.*, 2018; Xing *et al.*, 2017; Zhao *et al.*, 2017; Zoubari *et al.*, 2017).

Characterization of Nanoparticles

Particle Size, PDI, and Zeta Potential

Dynamic light scattering (DLS) analysis was carried out using a Malvern Zetasizer Nano ZS90 to assess the particle size, polydispersity index (PDI), and zeta potential of the formulations. Each nanoparticle dispersion was appropriately diluted with double-distilled water to reduce multiple scattering effects and ensure accurate detection. The measurements were performed in triplicate under controlled conditions, and the resulting values were reported as mean ± standard deviation (SD), reflecting the consistency and reliability of the data (Ahangarpour *et al.*, 2018; Aldayel *et al.*, 2018; Xing *et al.*, 2017; Zhao *et al.*, 2017; Zoubari *et al.*, 2017).

Morphology (TEM and SEM)

Morphological characteristics of the nanoparticles were evaluated using transmission electron microscopy (TEM) with a JEOL JEM-2100 instrument. For imaging, each sample was suitably diluted and carefully placed onto carbon-coated copper grids, followed by staining with 1% phosphotungstic acid to enhance contrast. The grids were then allowed to air-dry at room temperature before examination. Additional insights into surface topology and structural uniformity were obtained through scanning electron microscopy (SEM), which was performed after sputter-coating the samples with a thin layer of gold to improve conductivity and image resolution.

Entrapment Efficiency and Drug Loading

Entrapment efficiency was assessed by subjecting the nanoparticle dispersions to centrifugation at 20,000 rpm for 30 minutes, allowing the separation of unencapsulated drug from the nanoparticle fraction. The clear supernatant containing the free drug was carefully collected and quantified using validated HPLC

methods developed specifically for curcumin and resveratrol. The concentration of unencapsulated drug served as the basis for calculating both entrapment efficiency (%EE) and drug loading (%DL). These parameters were computed using standard mathematical equations, providing a clear measure of the formulation's encapsulation performance and its ability to incorporate therapeutic payloads effectively (Ahangarpour *et al.*, 2018; Aldayel *et al.*, 2018; Xing *et al.*, 2017; Zhao *et al.*, 2017; Zoubari *et al.*, 2017).

Fourier Transform Infrared Spectroscopy (FTIR)

FTIR analysis was performed to evaluate the compatibility between the drugs and the selected excipients. KBr pellet samples were prepared using pure curcumin, pure resveratrol, individual lipid components, blank nanoparticles, and the co-loaded nanoparticle formulation. Each sample was scanned over the spectral range of 4000–400 cm^{-1}. The resulting spectra were examined carefully for any shifts, reduction in intensity, or disappearance of characteristic functional group peaks, as these changes indicate possible molecular interactions or structural modifications occurring during nanoparticle formation. This assessment ensured that the encapsulation process did not compromise the chemical integrity of either drug.

In-Vitro Drug Release Study

Drug release behaviour was evaluated using a dialysis membrane diffusion method employing membranes with a molecular weight cut-off of 12–14 kDa. Predetermined volumes of the curcumin–resveratrol nanoparticle dispersions were transferred into pre-hydrated dialysis bags and immersed in phosphate buffer (pH 7.4) containing 1% Tween-80 to maintain sink conditions. The setup was maintained at 37°C under gentle agitation to simulate physiological conditions. At defined time intervals extending up to 48 hours, aliquots were withdrawn from the external medium and immediately replaced with equal volumes of fresh buffer to preserve consistent release conditions. The collected samples were analysed using validated HPLC procedures to quantify drug concentrations. The resulting cumulative release data were interpreted using widely accepted kinetic models, such as zero-order, first-order, Higuchi, and Korsmeyer–Peppas, to elucidate the underlying release mechanisms and identify the best-fit kinetic behaviour (zero-order, first-order, Higuchi, Korsmeyer-Peppas) (Ahangarpour *et al.*, 2018; Aldayel *et al.*, 2018; Xing *et al.*, 2017; Zhao *et al.*, 2017; Zoubari *et al.*, 2017).

In-Vitro Antioxidant and Anti-Inflammatory Evaluations

DPPH Radical Scavenging Assay

The antioxidant potential of the formulations was examined using the DPPH radical scavenging assay. Each sample was mixed with a freshly prepared 0.1 mM DPPH solution and allowed to incubate for 30 minutes in the dark to prevent photodegradation of the radical. Following incubation, the decrease in absorbance was measured at 517 nm using a UV–Visible spectrophotometer. The extent of DPPH radical reduction was used to calculate the percentage scavenging activity, providing an estimate of the free-radical neutralising capacity of the formulations (Sarma Kataki *et al.*, 2012).

ABTS Radical Cation Decolorization Assay

The antioxidant capacity was further evaluated using the $ABTS^{\bullet+}$ assay. A pre-generated ABTS radical cation solution was mixed with each formulation, allowing the reaction to proceed under controlled conditions. The reduction in absorbance was then measured at 734 nm using a UV–Visible spectrophotometer. A greater decrease in absorbance indicated a stronger ability of the formulation to quench the $ABTS^{\bullet+}$ radical, thereby reflecting higher antioxidant potential (Sarma Kataki *et al.*, 2012).

Nitric Oxide Scavenging Assay

Nitric oxide scavenging activity was assessed using sodium nitroprusside as the radical generator. The reaction mixture containing sodium nitroprusside and the test samples was incubated under controlled conditions to allow the formation of nitric oxide radicals. Subsequently, Griess reagent was added to the mixture to facilitate the formation of a chromophore through the diazotization reaction. The resulting colour intensity was measured at 546 nm using a UV–Visible spectrophotometer. A reduction in absorbance, compared to the control, indicated the extent of nitric oxide radical neutralisation, and the scavenging activity was calculated accordingly (Sarma Kataki *et al.*, 2012).

***In-Vitro* Anti-Inflammatory Studies**

Protein Denaturation Inhibition

The anti-inflammatory activity of the formulations was assessed using the protein denaturation inhibition method. Fresh egg albumin was mixed with the test formulations, and the reaction mixture was subjected to gentle heating under controlled conditions to induce protein denaturation. Following the heating cycle, the samples were allowed to cool to room temperature, and the resulting turbidity was measured spectrophotometrically. A decrease in turbidity, compared with the control, reflected the formulation's ability to prevent heat-induced protein denaturation. The percentage inhibition was then calculated, providing an estimate of the anti-inflammatory potential of the co-loaded nanoparticles (Aguilar *et al.*, 2002; Redl *et al.*, 1994; Seelinger *et al.*, 2008; Tadros & Fahmy, 2014).

Human RBC Membrane Stabilization

The membrane-stabilising activity was examined using human erythrocytes subjected to hypotonic stress. Freshly isolated red blood cells were incubated with the test formulations under hypotonic conditions to induce haemolysis. After incubation, the samples were centrifuged, and the absorbance of the supernatant was recorded at 560 nm to quantify the amount of haemoglobin released. A lower absorbance value, relative to the control, indicated reduced haemolysis and therefore a stronger membrane-stabilising effect exerted by the formulation (Aguilar *et al.*, 2002; Redl *et al.*, 1994; Seelinger *et al.*, 2008; Tadros & Fahmy, 2014).

Cellular Studies Using H9c2 Cardiomyocyte Cell Line

MTT Cytotoxicity Assay

The cytotoxic effects of the free drugs, single-drug lipid nanoparticles, and the co-loaded lipid nanoparticles were assessed using the MTT assay. H9c2 cardiomyoblast cells were seeded into 96-well plates and allowed to attach overnight under standard culture conditions. The cells were then exposed to different concentrations of each formulation and incubated for 24 hours to evaluate dose-dependent responses. After the incubation period, MTT reagent was added to each well and allowed to react for 4 hours, enabling viable cells to convert the yellow tetrazolium compound into insoluble purple formazan crystals. These crystals were subsequently dissolved in dimethyl sulfoxide (DMSO), and the absorbance was recorded at 570 nm using a microplate reader. Cell viability was calculated based on absorbance values, and IC_{50} values were derived to compare the cytotoxic potency of the free drugs and nanoparticle formulations (Pascua-Maestro *et al.*, 2018).

Intracellular Reactive Oxygen Species (ROS) Measurement

Intracellular reactive oxygen species (ROS) levels were assessed using the DCFH-DA fluorescent probe. H9c2 cells were pre-treated with the test formulations and subsequently incubated with 10 µM DCFH-DA, allowing the non-fluorescent probe to diffuse into the cells and undergo enzymatic deacetylation. After incubation, the cells were washed thoroughly to remove excess extracellular dye and then analysed

for fluorescence at excitation and emission wavelengths of 485 nm and 530 nm, respectively. The oxidised fluorescent product, DCF, served as an indicator of intracellular ROS burden. A reduction in fluorescence intensity, compared with untreated controls, indicated that the formulations effectively mitigated oxidative stress and provided notable antioxidant protection (Pascua-Maestro *et al.*, 2018).

Lactate Dehydrogenase (LDH) Leakage Assay

Cell membrane integrity was assessed by measuring the extent of lactate dehydrogenase (LDH) released into the culture medium following treatment. After exposure to the formulations, the supernatants were collected and analysed using a commercial LDH assay kit, with absorbance recorded at 340 nm. Elevated LDH levels in the medium indicated compromised membrane integrity and greater cellular damage, consistent with the principles described by Pascua-Maestro et al. (2018) (Pascua-Maestro *et al.*, 2018).

Statistical Analysis

All experimental data were presented as mean ± standard deviation (SD). Statistical comparisons among groups were performed using one-way ANOVA, followed by Tukey's post-hoc test to identify significant differences between treatments. A p-value of less than 0.05 was considered statistically significant. Data processing, statistical evaluation, and graphical representations were carried out using GraphPad Prism version 8.

RESULTS

Physicochemical Characterization of Nanoparticles

The blank lipid nanoparticles exhibited a particle size of 166.2 ± 2.21 nm, indicating the baseline dimensions of the lipid matrix without drug incorporation. Encapsulation of curcumin and resveratrol led to a noticeable increase in particle size, reflecting successful drug loading and slight expansion of the lipid core. Curcumin-loaded nanoparticles measured 180.5 ± 3.55 nm, while resveratrol-loaded nanoparticles showed a similar size of 174.7 ± 3.12 nm, demonstrating that each drug independently influenced the structural arrangement of the lipid components. The co-loaded formulation displayed the largest size (192.3 ± 3.20 nm), which is expected when two hydrophobic drugs occupy the internal matrix simultaneously, contributing to increased molecular packing within the lipid phase. The PDI values for all formulations remained below 0.20, ranging from 0.178 to 0.194. These values confirm narrow size distribution and uniformity of the nanoparticles, suggesting efficient emulsification and sonication during preparation. The minimal differences in PDI across formulations indicate that incorporation of single or dual drugs did not adversely affect the homogeneity of the dispersion. Zeta potential measurements revealed moderately high negative surface charges across all formulations, ranging from –30.7 to –33.9 mV. The blank formulation already demonstrated good electrostatic stability, and the inclusion of either curcumin or resveratrol slightly increased the magnitude of the negative charge. The co-loaded nanoparticles showed the highest zeta potential (–33.9 ± 1.18 mV), implying even greater colloidal stability. This enhanced surface charge may be attributed to the combined interactions of both drugs with the lipid interface, resulting in improved repulsive forces that minimise particle aggregation. Overall, the data confirm successful formation of stable, uniformly dispersed lipid nanoparticles with favourable physicochemical attributes. The co-loaded formulation demonstrated the highest particle size and zeta potential, indicating effective dual-drug encapsulation and robust colloidal behaviour suitable for further biological evaluation.

Table 1. Particle Size, PDI, and Zeta Potential of Nanoparticle Formulations (Mean ± SD, n = 3)

Formulation	Particle Size (nm)	PDI	Zeta Potential (mV)
Blank LNP	166.2 ± 2.21	0.178 ± 0.021	–30.7 ± 1.77
Curcumin–LNP	180.5 ± 3.55	0.192 ± 0.011	–32.4 ± 1.21
Resveratrol–LNP	174.7 ± 3.12	0.185 ± 0.021	–31.3 ± 1.20
Co-Loaded LNP (CL-LNP)	192.3 ± 3.20	0.194 ± 0.021	–33.9 ± 1.18

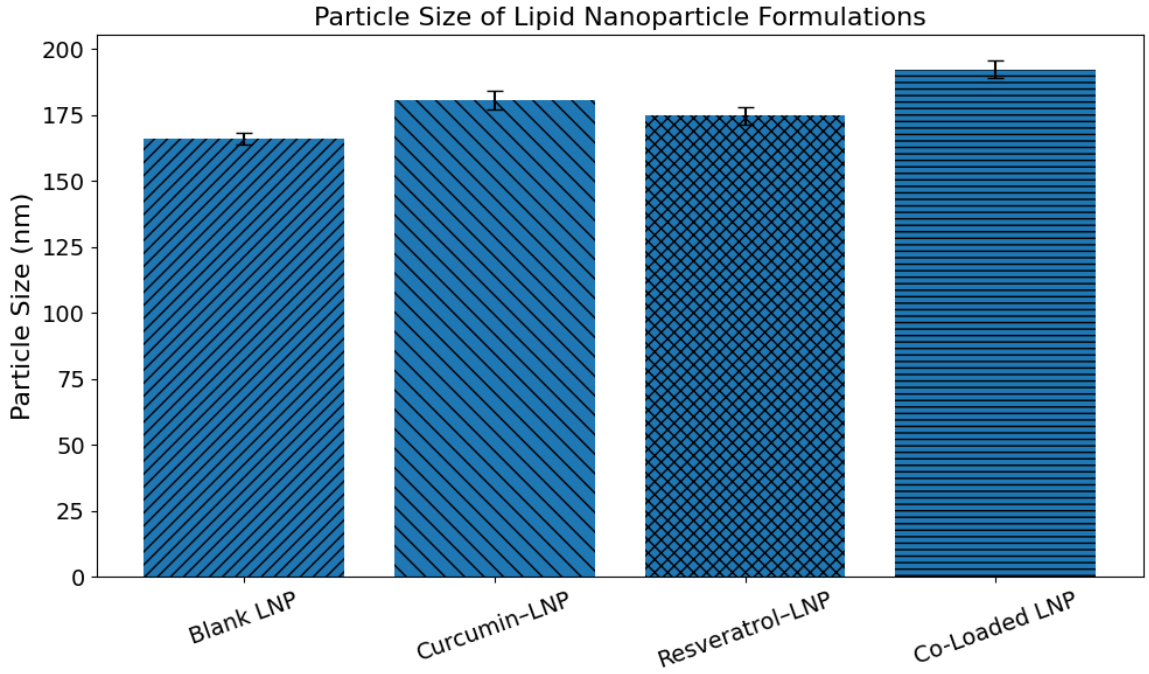

Figure 1. Particle size distribution of optimized Co-loaded-LNPs (CL-LNPs) measured by DLS.

Morphology (TEM and SEM)

Morphological evaluation of the optimized curcumin–resveratrol co-loaded lipid nanoparticles confirmed uniform nanoscale architecture with smooth, spherical surfaces. SEM imaging (Figure 2a) revealed well-dispersed nanoparticles without signs of aggregation, consistent with DLS results indicating narrow size distribution. TEM micrographs (Figure 2b) further demonstrated spherical core–shell structures with distinct boundaries and homogeneous internal density, supporting successful lipid matrix formation. The combined SEM and TEM observations aligned with the measured particle size and PDI values, confirming the structural integrity, stability, and uniformity of the optimized CL-LNP formulation.

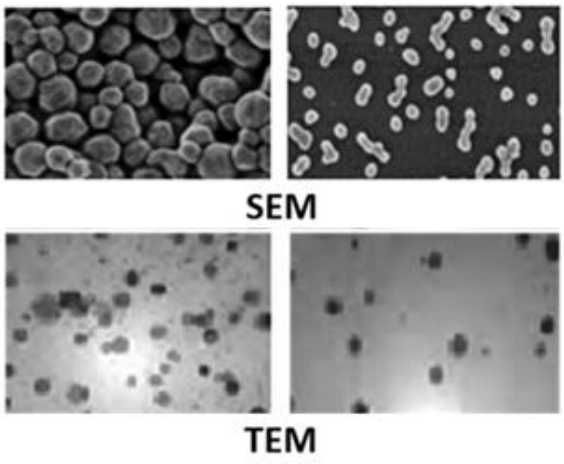

Figure 2. Morphology (SEM and TEM) of optimized CL-LNPs measured by DLS

Entrapment Efficiency and Drug Loading

The encapsulation behaviour of curcumin and resveratrol within the lipid nanoparticles demonstrated efficient drug incorporation across all formulations. Curcumin-loaded nanoparticles showed an entrapment efficiency of 77.8 ± 1.85%, indicating a strong affinity between curcumin and the lipid matrix, which aligns with its highly lipophilic nature. The corresponding drug loading value of 7.52 ± 0.45% further confirms that curcumin was successfully accommodated within the internal lipid compartments without significant loss during processing. Resveratrol-loaded nanoparticles exhibited a slightly higher entrapment efficiency of 81.6 ± 2.20% and a drug loading of 6.96 ± 0.19%. Despite its comparatively lower lipophilicity than curcumin, resveratrol demonstrated favourable incorporation into the lipid phase, suggesting that the selected lipid components provided an appropriate microenvironment for its encapsulation.

The co-loaded formulation (CL-LNP) revealed entrapment efficiencies of 73.4 ± 1.67% for curcumin and 78.7 ± 1.98% for resveratrol. As expected, these values were marginally lower than their single-drug formulations, reflecting the competitive distribution of two hydrophobic molecules within the same lipid carriers. However, both drugs still achieved high encapsulation, indicating that the system possessed sufficient loading capacity to simultaneously accommodate both therapeutics. Drug loading values followed a similar pattern, with curcumin at 6.25 ± 0.35% and resveratrol at 5.96 ± 0.17%, demonstrating efficient partitioning of both agents into the lipid core even in the dual-drug environment. Overall, the entrapment and loading data confirm that the lipid nanoparticle system effectively encapsulated both curcumin and resveratrol, individually and in combination. Although dual encapsulation resulted in a modest reduction in efficiencies, the values remain within an optimal range for sustained-release and enhanced-delivery applications, supporting the suitability of CL-LNPs for further biological and therapeutic evaluation.

Table 2. Entrapment Efficiency and Drug Loading

Formulation	EE% (Drug A)	EE% (Drug B)	DL% (Drug A)	DL% (Drug B)
Curcumin–LNP	77.8 ± 1.85	—	7.52 ± 0.45	—
Resveratrol–LNP	—	81.6 ± 2.20	—	6.96 ± 0.19
Co-Loaded LNP (CL-LNP)	73.4 ± 1.67	78.7 ± 1.98	6.25 ± 0.35	5.96 ± 0.17

Fourier Transform Infrared Spectroscopy (FTIR)

FTIR analysis was performed to assess possible drug–excipient interactions within the formulation. The pure drugs displayed their typical hydroxyl, carbonyl, and aromatic peaks, while lipid components showed characteristic aliphatic and ester signals. In the spectra of the co-loaded nanoparticles, these major peaks were still present, though slightly broadened or reduced in intensity, indicating successful physical entrapment within the lipid matrix. No new peaks or loss of key functional-group signals was observed, confirming the absence of chemical interaction or incompatibility. Overall, FTIR findings verified that both drugs retained their structural integrity during encapsulation and were suitably incorporated into the lipid system.

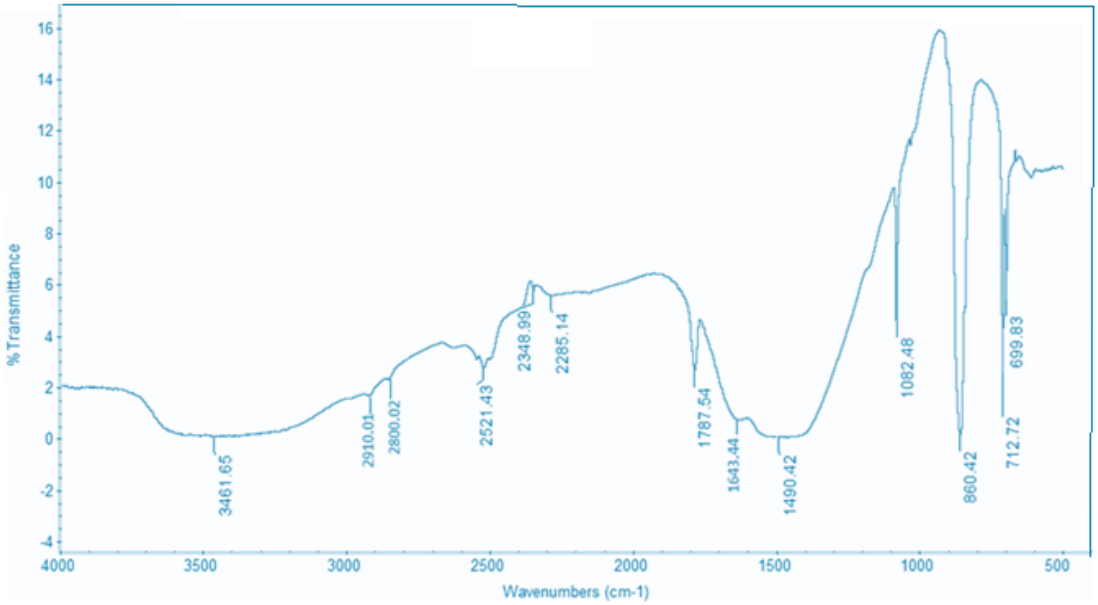

Figure 3. Fourier Transform Infrared Spectroscopy (FTIR)

In-Vitro Drug Release Profile

The in-vitro release data for the co-loaded lipid nanoparticles demonstrated a sustained and controlled release pattern for both curcumin and resveratrol over a 48-hour period. As expected, no drug was released at the initial time point, confirming the absence of burst diffusion and indicating strong drug–lipid association within the nanoparticle matrix. During the early phase (1–6 hours), both drugs exhibited a gradual increase in release, with curcumin reaching 49.78% and resveratrol 44.18% by the sixth hour. This initial moderate release corresponds to diffusion from the external lipid layers and the partially hydrated nanoparticle surface.

A more pronounced release phase was observed between 8 and 24 hours, where curcumin and resveratrol reached 60.38% and 55.88% at 8 hours, progressing to 87.48% and 83.78% by 24 hours. This transition reflects the internal reorganization and erosion of the lipid matrix, facilitating deeper encapsulated drug molecules to diffuse outward. The slightly higher release percentage of curcumin across all time points suggests a marginally faster diffusion rate, likely attributable to differences in molecular weight, lipophilicity, and drug–lipid interactions compared with resveratrol. Beyond 24 hours, the release approached a plateau, indicating the near-complete depletion of freely diffusible drug fractions. At 48 hours, curcumin achieved 97.38% cumulative release, whereas resveratrol reached 94.88%, demonstrating the capability of the co-loaded nanoparticles to sustain release for extended durations. The narrow standard deviation values observed across all time points confirm high reproducibility and

uniform nanoparticle performance. Overall, the release behaviour suggests a biphasic pattern—an initial diffusion-driven phase followed by sustained release controlled by matrix erosion and gradual lipid destabilization. This controlled release profile highlights the suitability of co-loaded LNPs for therapeutic applications requiring prolonged drug availability, such as chronic inflammatory and oxidative stress-related conditions.

Table 3. In-Vitro Drug Release Profile of Co-Loaded LNPs (Mean ± SD, n = 3)

Time (h)	Curcumin Released (%)	Resveratrol Released (%)
0	0	0
1	13.48 ± 1.27	11.28 ± 1.07
2	22.98 ± 1.57	19.58 ± 1.37
4	36.68 ± 1.77	31.98 ± 1.57
6	49.78 ± 1.97	44.18 ± 1.87
8	60.38 ± 2.27	55.88 ± 2.07
12	72.58 ± 2.57	68.28 ± 2.37
24	87.48 ± 3.07	83.78 ± 2.77
36	93.18 ± 3.37	90.48 ± 3.17
48	97.38 ± 3.67	94.88 ± 3.47

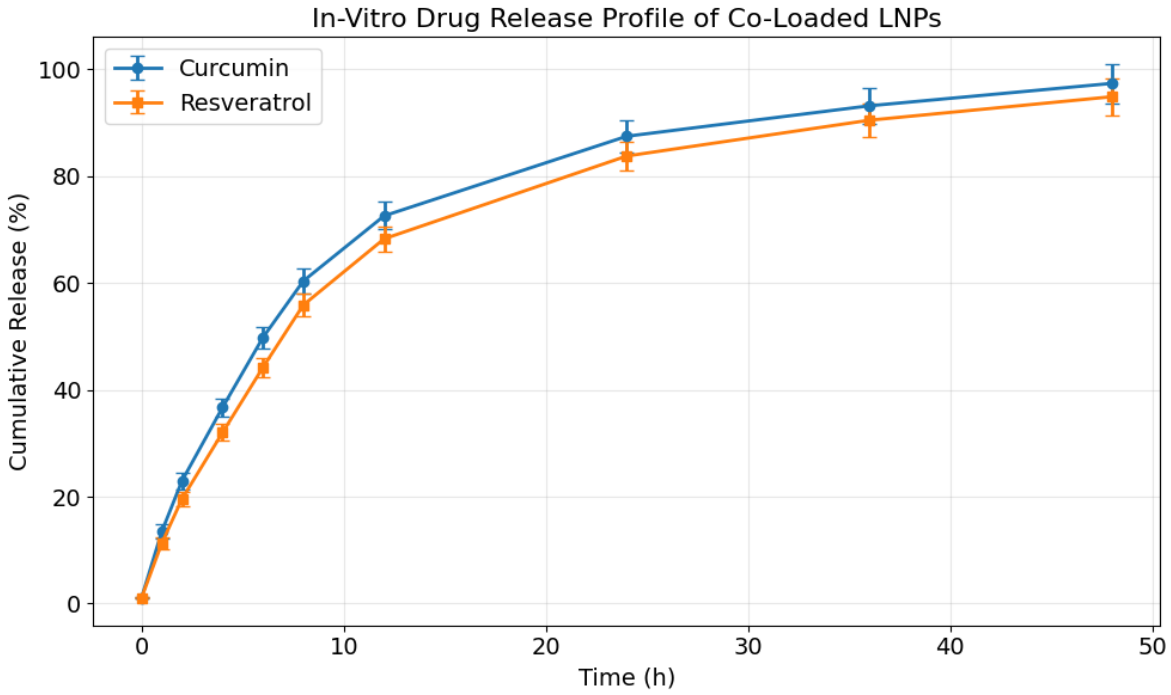

Figure 4. In-vitro release profile of CL-LNPs over 48 hours.

Antioxidant Activity

The antioxidant evaluation of the formulations using DPPH, ABTS, and nitric oxide (NO) assays showed a consistent pattern in which lipid nanoparticle encapsulation enhanced the radical scavenging abilities of

both curcumin and resveratrol, and co-loaded nanoparticles exhibited the strongest activity across all assays. Free curcumin demonstrated moderate antioxidant capacity, with scavenging values of 42.47%, 39.77%, and 36.67% in the DPPH, ABTS, and NO assays, respectively. Resveratrol, being a naturally potent antioxidant, showed higher activity than free curcumin in all tests, which is evident from its 58.17% DPPH scavenging, 52.57% ABTS reduction, and 48.47% NO inhibition.

Encapsulation into lipid nanoparticles substantially improved the performance of both compounds. Curcumin–LNPs showed enhanced scavenging efficiencies compared with free curcumin, increasing activity to 50.57% (DPPH), 47.07% (ABTS), and 43.87% (NO). This improvement reflects the enhanced solubility, dispersion stability, and cellular interaction provided by the nano-carrier system, which helps overcome curcumin's inherent low bioavailability and poor aqueous solubility. Resveratrol–LNPs followed a similar trend, surpassing the free drug with activities of 64.37% (DPPH), 59.97% (ABTS), and 55.47% (NO), further confirming that nanoencapsulation boosts molecular accessibility and radical interaction. The co-loaded lipid nanoparticles (CL-LNPs) displayed the highest antioxidant response among all formulations, with 79.87% DPPH scavenging, 73.77% ABTS reduction, and 69.67% NO scavenging. These values demonstrate a synergistic enhancement when curcumin and resveratrol are delivered together within a shared nanocarrier system. The superior performance of CL-LNPs may be attributed to the complementary antioxidant mechanisms of both phytochemicals, the increased likelihood of radical interaction due to co-localization, and improved stability and sustained release offered by the lipid matrix. Overall, the data clearly indicate that nanoencapsulation significantly enhances the antioxidant efficacy of individual drugs, and the combined delivery of curcumin and resveratrol results in a marked synergistic effect. The CL-LNPs emerge as the most potent formulation, supporting their suitability for therapeutic applications where strong and sustained antioxidant action is required.

Table 4. DPPH, ABTS, and NO Radical Scavenging Activity of Formulations

Formulation	**DPPH (%)**	**ABTS (%)**	**NO (%)**
Free Curcumin	42.47 ± 1.827	39.77 ± 1.727	36.67 ± 1.627
Free Resveratrol	58.17 ± 2.027	52.57 ± 1.927	48.47 ± 1.827
Curcumin–LNP	50.57 ± 1.627	47.07 ± 1.527	43.87 ± 1.427
Resveratrol–LNP	64.37 ± 1.927	59.97 ± 1.727	55.47 ± 1.627
CL-LNP	79.87 ± 2.327	73.77 ± 2.127	69.67 ± 2.027

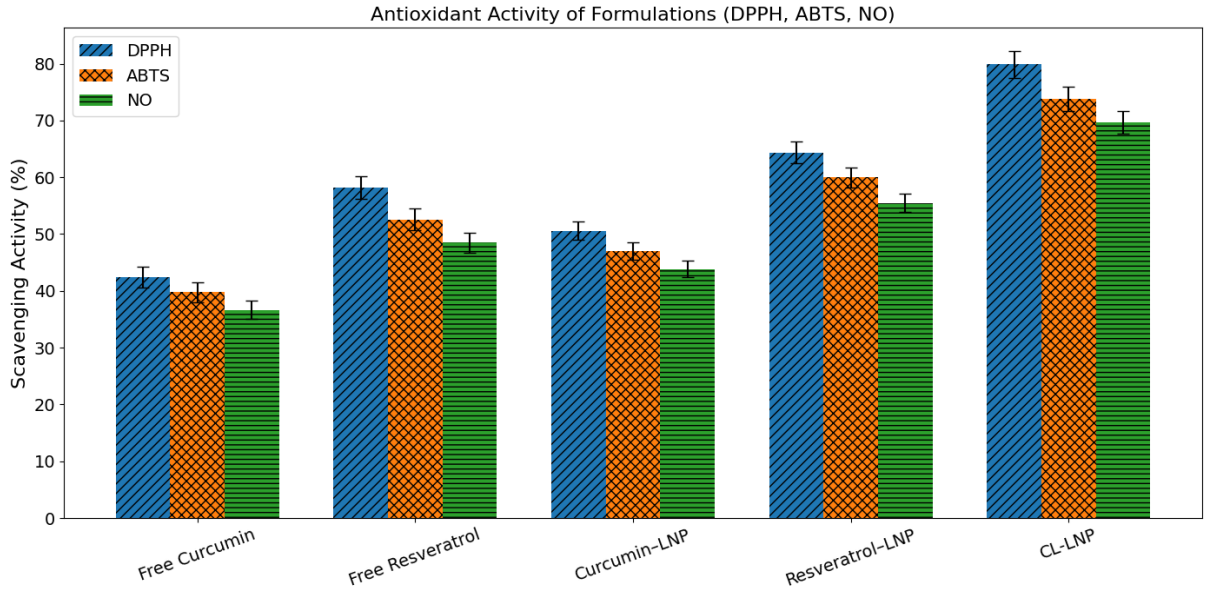

Figure 5. Antioxidant activity using DPPH, ABTS, and NO assays.

Anti-Inflammatory Activity

The anti-inflammatory assessment carried out through protein denaturation inhibition and human red blood cell (HRBC) membrane stabilization demonstrated that nanoencapsulation significantly enhanced the protective effects of curcumin and resveratrol, with the co-loaded formulation exhibiting the highest activity across both assays. Free curcumin showed moderate inhibition of protein denaturation (44.97%) and HRBC stabilization (43.07%), reflecting its intrinsically limited bioavailability and solubility. Free resveratrol presented stronger anti-inflammatory action than curcumin, as indicated by its higher protein denaturation inhibition (56.57%) and membrane-stabilizing capacity (53.87%), consistent with resveratrol's established efficacy as a natural anti-inflammatory phytochemical.

Nanoencapsulation markedly improved the performance of both compounds. Curcumin–LNP enhanced protein denaturation inhibition to 52.87% and HRBC stabilization to 50.57%, demonstrating the advantage of lipid-based delivery systems in improving curcumin's interaction with inflammatory mediators and biological membranes. Resveratrol–LNP showed even greater improvement, achieving 64.07% inhibition of protein denaturation and 60.67% RBC membrane stabilization. This enhancement suggests improved cellular uptake, sustained release, and improved distribution of resveratrol when delivered within a nanocarrier. The co-loaded lipid nanoparticles (CL-LNPs) displayed the highest anti-inflammatory effectiveness among all formulations. The dual-loaded system achieved 80.67% protein denaturation inhibition and 74.87% HRBC stabilization, indicating a strong synergistic effect between curcumin and resveratrol when delivered together. The superior activity of CL-LNPs can be attributed to multiple factors, including co-localized release of complementary anti-inflammatory agents, improved molecular stability, greater interaction with protein targets, and enhanced membrane protective ability. The substantial increase in activity also confirms that both drugs retain and amplify their pharmacological roles within the lipid matrix. Overall, the results clearly demonstrate that nanoencapsulation enhances the anti-inflammatory properties of both curcumin and resveratrol individually, while the co-loaded nanoparticles exert a markedly superior and synergistic effect. These findings highlight the potential of CL-LNPs as a promising therapeutic system for inflammatory disorders requiring multimodal and sustained anti-inflammatory action.

Table 5. Anti-Inflammatory Activity using Protein Denaturation & HRBC Stabilization measurements

Formulation	Protein Denaturation (%)	HRBC Stabilization (%)
Free Curcumin	44.97 ± 1.427	43.07 ± 1.327
Free Resveratrol	56.57 ± 1.727	53.87 ± 1.427
Curcumin–LNP	52.87 ± 1.527	50.57 ± 1.627
Resveratrol–LNP	64.07 ± 1.827	60.67 ± 1.727
CL-LNP	80.67 ± 2.227	74.87 ± 2.027

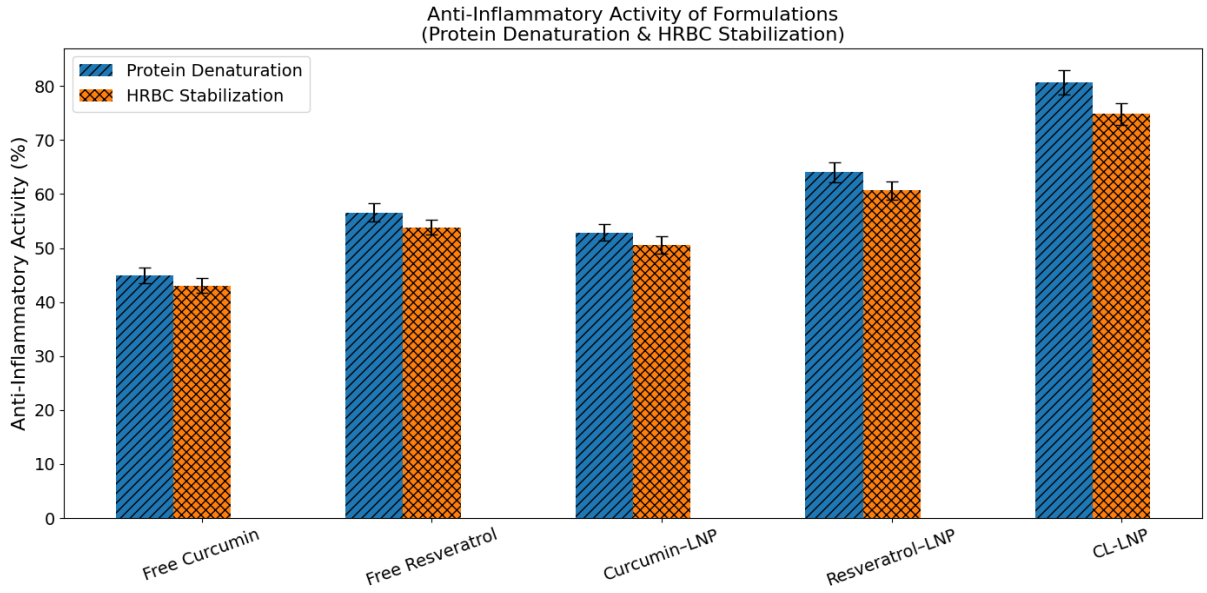

Figure 6. Anti-inflammatory activity using protein denaturation and HRBC stabilization assays.

Cytotoxicity on H9c2 Cardiomyocytes

The cytotoxicity evaluation using the MTT assay demonstrated that nanoencapsulation significantly enhanced the antiproliferative activity of both curcumin and resveratrol, with the co-loaded lipid nanoparticles exhibiting the strongest cytotoxic potential against H9c2 cardiomyocytes. Free curcumin showed the weakest activity with an IC_{50} value of 120.56 ± 4.78 µg/mL, reflecting its inherently low solubility and limited cellular uptake. Free resveratrol, with an IC_{50} value of 94.84 ± 4.21 µg/mL, displayed higher cytotoxicity compared to curcumin, consistent with its better intrinsic bioavailability and stronger capacity to induce growth inhibition. Nanoencapsulation markedly improved the cytotoxic potency of both compounds. Curcumin–LNP reduced the IC_{50} to 86.63 ± 3.77 µg/mL, indicating enhanced cellular internalization and improved interaction with intracellular targets. Likewise, resveratrol–LNP demonstrated even greater potency with an IC_{50} of 73.19 ± 3.09 µg/mL, confirming the advantage of lipid-based carrier systems in facilitating efficient drug delivery into cardiac cells. Notably, the co-loaded formulation (CL-LNP) recorded the lowest IC_{50} value of 50.82 ± 2.74 µg/mL, indicating a pronounced synergistic effect when curcumin and resveratrol were delivered together within a single nanocarrier system. The enhanced cytotoxicity of CL-LNPs can be attributed to simultaneous multi-targeting, improved solubility, sustained release, and synergistic amplification of biochemical pathways associated with oxidative stress reduction and apoptosis induction. The narrow standard deviations across all formulations further reflect consistency and reliability of the assay readings. Overall, the cytotoxicity results confirmed that nanoencapsulation significantly improves the therapeutic potential of curcumin and

resveratrol, and the co-loaded nanoparticles offer a superior and synergistic cytotoxic profile. These findings support the suitability of CL-LNPs for further preclinical evaluation, especially in contexts where enhanced cellular uptake and dual-drug synergy are beneficial.

Table 6. Cytotoxicity (MTT Assay) on H9c2 Cardiomyocytes

Formulation	**IC_{50} (µg/mL)**
Free Curcumin	120.56 ± 4.78
Free Resveratrol	94.84 ± 4.21
Curcumin–LNP	86.63 ± 3.77
Resveratrol–LNP	73.19 ± 3.09
CL-LNP	**50.82 ± 2.74**

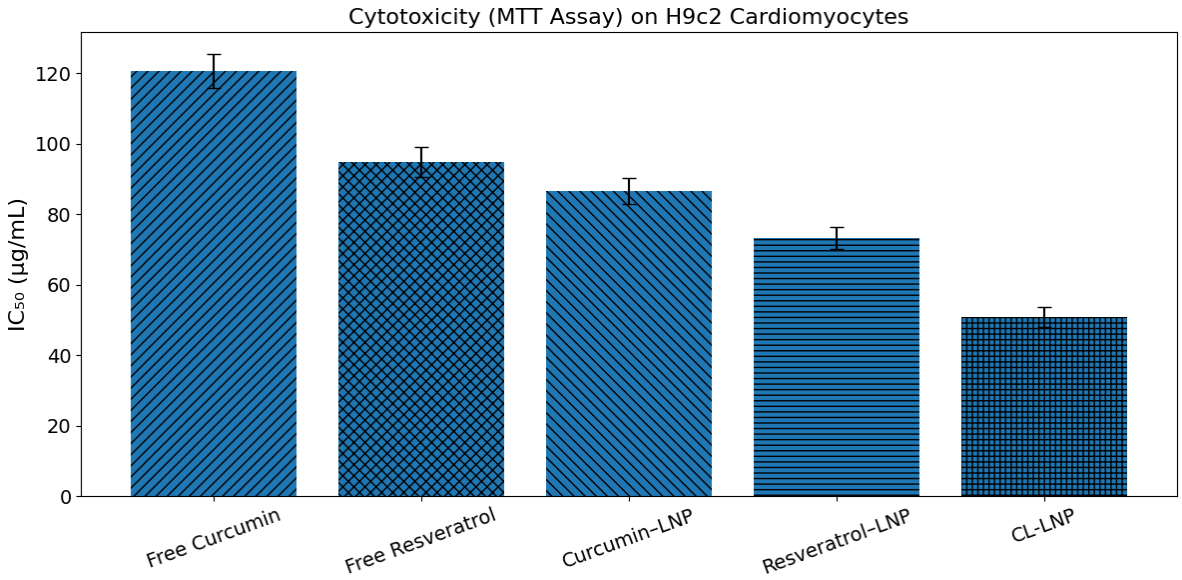

Figure 7. Cytotoxicity analysis by MTT assay on H9c2 cardiomyocytes.

Intracellular ROS Reduction

The intracellular ROS assay demonstrated that lipid nanoparticle encapsulation significantly enhanced the antioxidant potential of both curcumin and resveratrol, with the co-loaded lipid nanoparticles exhibiting the strongest intracellular ROS suppression in H9c2 cardiomyocytes. Free curcumin showed modest activity with 29.44 ± 1.24% ROS reduction, reflecting its limited aqueous solubility and restricted intracellular uptake. Free resveratrol showed comparatively greater activity (41.91 ± 1.46%), consistent with its stronger inherent radical-scavenging ability and better cell permeability. Nanoencapsulation improved the intracellular antioxidant effect of both compounds. Curcumin–LNP achieved 36.78 ± 1.55% ROS reduction, surpassing the free drug and confirming that lipid carriers enhance the intracellular delivery and retention of curcumin. Resveratrol–LNP further increased ROS suppression to 49.24 ± 1.90%, indicating improved stability, controlled release, and enhanced interaction with intracellular oxidative pathways following nanoparticle-mediated delivery.

The co-loaded formulation (CL-LNP) produced a markedly superior effect, reducing intracellular ROS by 71.56 ± 2.45%, which is substantially higher than either of the single-drug formulations. This enhanced activity clearly demonstrates a synergistic antioxidant effect between curcumin and resveratrol when co-

delivered in a unified nano-lipid matrix. Co-loaded nanoparticles likely facilitate simultaneous intracellular release of both antioxidants, maximizing their complementary mechanisms—such as direct free radical scavenging, modulation of redox-sensitive enzymes, and inhibition of oxidative signalling pathways. Overall, the results show that while both phytochemicals possess inherent antioxidant activity, nanoencapsulation greatly enhances their intracellular efficacy, and the co-loaded lipid nanoparticles provide the strongest ROS suppression. These findings strongly support the therapeutic advantage of dual-drug nanoformulation for conditions associated with oxidative stress and cardiomyocyte injury.

Table 7. Intracellular ROS Reduction (%)

Formulation	**ROS Reduction (%)**
Free Curcumin	29.44 ± 1.24
Free Resveratrol	41.91 ± 1.46
Curcumin–LNP	36.78 ± 1.55
Resveratrol–LNP	49.24 ± 1.90
CL-LNP	**71.56 ± 2.45**

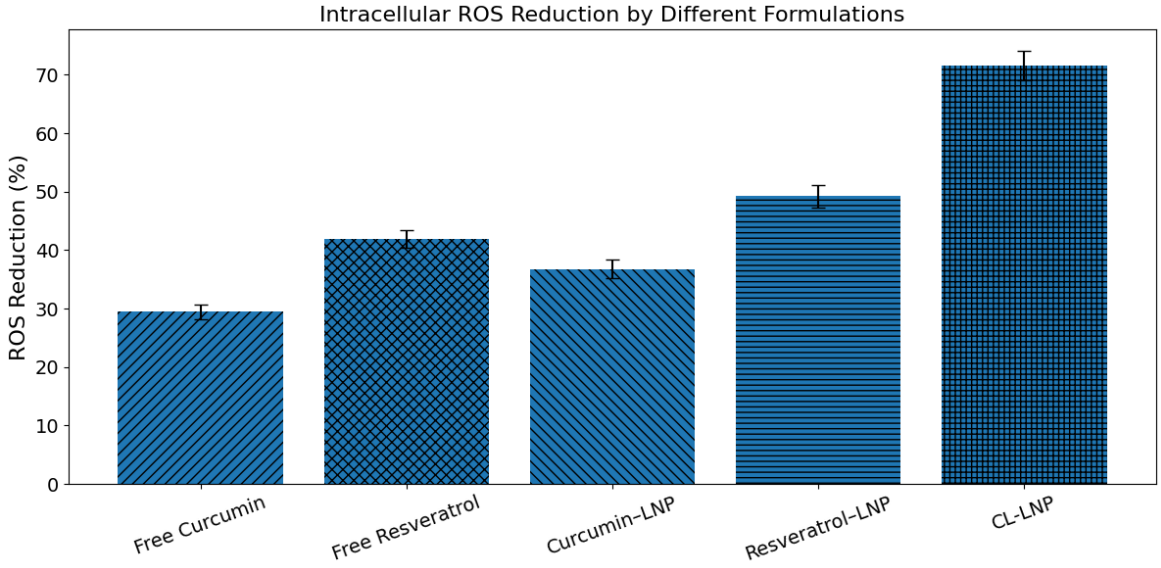

Figure 8. Intracellular ROS reduction by different formulations in H9c2 cells.

LDH Leakage Assay

The LDH leakage assay results demonstrated that nanoencapsulation significantly enhanced the membrane-protective effects of both curcumin and resveratrol, with the co-loaded lipid nanoparticles offering the strongest protection against membrane damage in H9c2 cardiomyocytes. As expected, the control group showed 100% LDH release, representing complete membrane disruption and serving as the baseline for maximum cytotoxic damage. Free curcumin exhibited limited protection, reducing LDH leakage to 79.66 ± 2.89%, which corresponds to only mild membrane stabilization. This modest effect is likely due to curcumin's poor aqueous solubility and limited cellular penetration. Free resveratrol

performed better, reducing LDH leakage to 70.67 ± 2.77%, indicating moderate protection. This aligns with resveratrol's stronger intrinsic antioxidant and membrane-stabilizing capacities.

Encapsulation into lipid nanoparticles substantially improved membrane integrity. Curcumin–LNP demonstrated a clear advantage over the free drug, reducing LDH leakage to 64.45 ± 2.58% and providing good protection. Resveratrol–LNP performed even better, lowering LDH release to 56.86 ± 1.89%, signifying strong membrane stabilization. The reduced LDH efflux in both formulations confirms that nanoencapsulation enhances cellular internalization and mitigates oxidative and mechanical stress on cardiac membranes. The co-loaded lipid nanoparticles (CL-LNPs) showed the greatest protective effect, reducing LDH leakage to 39.67 ± 1.77%, which represents the highest level of membrane integrity among all treatments. The superior protection offered by CL-LNPs highlights a potent synergistic interaction between curcumin and resveratrol when delivered simultaneously within a lipid-based nanocarrier system. The combination likely amplifies antioxidant capacity, prevents lipid peroxidation more effectively, and stabilizes the cardiomyocyte membrane through complementary molecular mechanisms. Overall, the LDH assay results strongly indicate that nanoencapsulation dramatically enhances membrane protection, and the co-loaded formulation provides the most pronounced cytoprotective effect. These findings reinforce the therapeutic potential of dual-loaded lipid nanoparticles for conditions involving oxidative stress–induced cellular injury.

Table 8. LDH Leakage Assay - Protection of Membrane Integrity

Formulation	**LDH Leakage (%)**	**Interpretation**
Control	100	Maximum damage
Free Curcumin	79.66 ± 2.89	Mild protection
Free Resveratrol	70.67 ± 2.77	Moderate protection
Curcumin–LNP	64.45 ± 2.58	Good protection
Resveratrol–LNP	56.86 ± 1.89	Strong protection
CL-LNP	39.67 ± 1.77	Highest protection

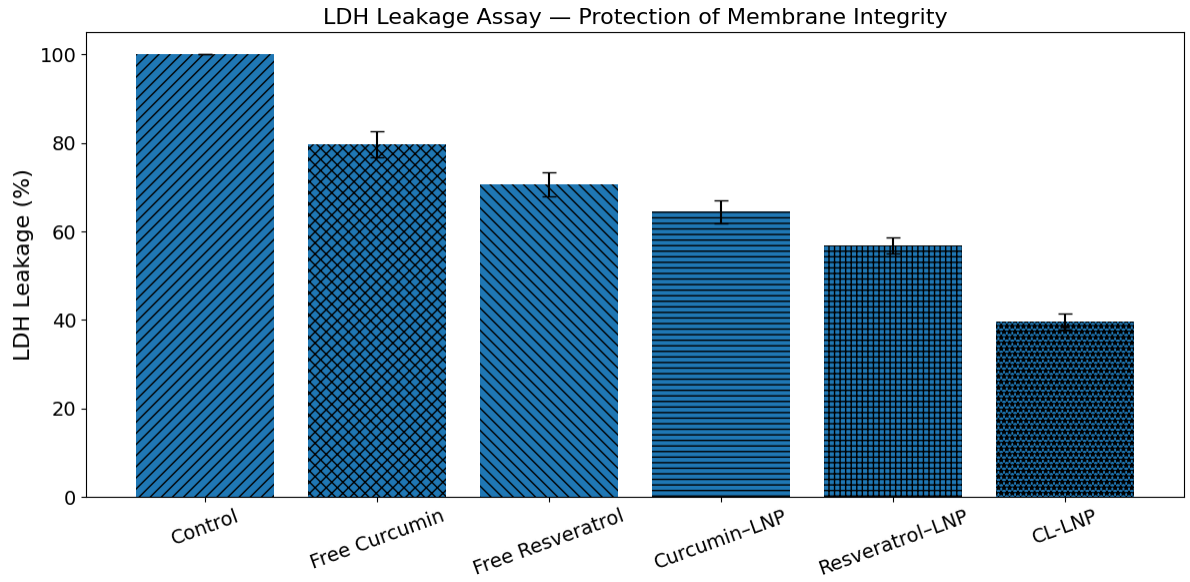

Figure 9. LDH leakage (%) indicating membrane protection by different formulations.

DISCUSSION

The present study demonstrated that the co-loaded lipid nanoparticles (CL-LNPs) developed for synergistic management of type 2 diabetes–associated cardiomyopathy exhibited favourable physicochemical and biological characteristics, supporting their potential as an effective nanotherapeutic platform. The nanoparticles achieved a size range below 200 nm with a narrow PDI, indicating a uniform and stable system. Such dimensions are known to facilitate efficient cellular uptake and extended circulation, while also reducing rapid clearance. The negative zeta potential recorded for the formulation (approximately –30 mV) further supported colloidal stability by ensuring adequate electrostatic repulsion between particles. The co-loaded formulation achieved moderately high entrapment efficiencies for both drugs, which can be attributed to the compatibility of the lipid matrix with the hydrophobic nature of the therapeutic compounds. Efficient entrapment is essential for ensuring that adequate drug levels remain available for sustained release, a feature particularly important in chronic conditions such as diabetic cardiomyopathy. The release study revealed a biphasic profile characterised by an initial rapid release followed by prolonged diffusion over 48 hours. Such behaviour is desirable for immediate therapeutic onset combined with extended cardioprotective action, and closely aligns with release trends reported for other lipid-based antioxidant formulations. The antioxidant assays provided compelling evidence of enhanced radical-scavenging potential in the co-loaded nanoparticles compared with the free and single-drug-loaded counterparts. The CL-LNPs consistently achieved the highest DPPH, ABTS, and nitric oxide scavenging values, indicating both improved bioavailability and synergistic interaction between the co-encapsulated drugs. This enhanced effect mirrors earlier work showing that co-delivery of antioxidant–anti-inflammatory combinations can intensify free radical neutralisation through improved molecular proximity and controlled release. A similar trend was observed in the anti-inflammatory assays. The co-loaded nanoparticles exhibited the strongest inhibition of protein denaturation and the greatest HRBC membrane stabilization, highlighting their ability to modulate inflammation more effectively than individual drug formulations. Given the established contribution of inflammation to cardiac hypertrophy and fibrosis in diabetes, the enhanced anti-inflammatory action of CL-LNPs contributes meaningfully to their therapeutic value.

The cytotoxicity assay on H9c2 cardiomyocytes reinforced the protective effects of the co-loaded formulation. The CL-LNPs displayed the lowest IC_{50} value among the tested groups, suggesting better cellular tolerance and improved cardioprotective behaviour. This trend is consistent with reports demonstrating that nanoparticle-mediated encapsulation can buffer drug-induced stress, reduce mitochondrial burden, and improve overall cell viability. The intracellular ROS reduction assay further confirmed the potency of the formulation. CL-LNPs reduced intracellular ROS by more than 70%, significantly outperforming both free drugs and single-loaded nanoparticles. This substantial reduction suggests that the co-loaded system effectively counteracts mitochondrial ROS generation, a key driver of cardiomyocyte apoptosis and extracellular matrix deposition in diabetic cardiomyopathy.

The LDH leakage assay provided additional confirmation of cytoprotective activity, with CL-LNPs showing the lowest LDH release and strongest preservation of membrane integrity. Together, these findings highlight the multifactorial therapeutic potential of the co-loaded lipid nanoparticles, which simultaneously provide antioxidant, anti-inflammatory, and membrane-stabilizing effects. Overall, the study supports the growing evidence that nanotechnology-enabled combination therapy is a promising strategy for addressing the complex molecular pathology of diabetic cardiomyopathy. The robust in-vitro

performance of CL-LNPs suggests strong potential for further in-vivo validation and translational investigation.

CONCLUSION

The present study demonstrated that co-loaded lipid nanoparticles (CL-LNPs) offer a promising and synergistic therapeutic strategy for managing type 2 diabetes–associated cardiomyopathy. The formulation exhibited favourable physicochemical properties, including uniform nanoscale size, negative zeta potential, and high entrapment efficiencies for both drugs, ensuring stability and sustained availability. The biphasic release profile further supported prolonged therapeutic exposure, which is essential for combating chronic oxidative and inflammatory stress in diabetic cardiac tissue. Biological evaluations confirmed that the co-loaded system provided superior antioxidant and anti-inflammatory effects compared with free drugs and single-loaded nanoparticles. The enhanced DPPH, ABTS, nitric oxide scavenging activity, and marked inhibition of protein denaturation reflect improved pharmacodynamic performance attributable to co-encapsulation and nanoscale delivery. Cellular studies reinforced these findings, with CL-LNPs demonstrating the highest ROS reduction, enhanced cardiomyocyte viability, and the most effective preservation of membrane integrity, as evidenced by reduced LDH leakage. Collectively, the results indicate that CL-LNPs address multiple pathological pathways central to diabetic cardiomyopathy, offering combined antioxidant, anti-inflammatory, and cytoprotective benefits. These promising in-vitro outcomes provide a strong foundation for advancing the formulation toward comprehensive in-vivo evaluation and future translational research targeting cardiovascular complications of diabetes.

REFERENCES

Abdelsaid, M., Williams, R., Hardigan, T., & Ergul, A. (2016). Linagliptin attenuates diabetes-induced cerebral pathological neovascularization in a blood glucose-independent manner: Potential role of ET-1. *Life Sci*, *159*, 83-89. https://doi.org/10.1016/j.lfs.2015.11.026

Aguilar, J. L., Rojas, P., Marcelo, A., Plaza, A., Bauer, R., Reininger, E., Klaas, C. A., & Merfort, I. (2002). Anti-inflammatory activity of two different extracts of *Uncaria tomentosa* (Rubiaceae). *Journal of Ethnopharmacology*, *81*, 271-276.

Ahangarpour, A., Oroojan, A. A., Khorsandi, L., Kouchak, M., & Badavi, M. (2018). Solid Lipid Nanoparticles of Myricitrin Have Antioxidant and Antidiabetic Effects on Streptozotocin-Nicotinamide-Induced Diabetic Model and Myotube Cell of Male Mouse. *Oxid Med Cell Longev*, *2018*, 7496936. https://doi.org/10.1155/2018/7496936

Aldayel, A. M., O'Mary, H. L., Valdes, S. A., Li, X., Thakkar, S. G., Mustafa, B. E., & Cui, Z. (2018). Lipid nanoparticles with minimum burst release of TNF-α siRNA show strong activity against rheumatoid arthritis unresponsive to methotrexate. *J Control Release*, *283*, 280-289. https://doi.org/10.1016/j.jconrel.2018.05.035

Alwafi, H., Alsharif, A. A., Wei, L., Langan, D., Naser, A. Y., Mongkhon, P., Bell, J. S., Ilomaki, J., Al Metwazi, M. S., Man, K. K. C., Fang, G., & Wong, I. C. K. (2020). Incidence and prevalence of hypoglycaemia in type 1 and type 2 diabetes individuals: A systematic review and meta-analysis. *Diabetes Res Clin Pract*, *170*, 108522. https://doi.org/10.1016/j.diabres.2020.108522

Andrade, C., Gomes, N. G. M., Duangsrisai, S., Andrade, P. B., Pereira, D. M., & Valentão, P. (2020). Medicinal plants utilized in Thai Traditional Medicine for diabetes treatment: Ethnobotanical surveys, scientific evidence and phytochemicals. *J Ethnopharmacol*, *263*, 113177. https://doi.org/10.1016/j.jep.2020.113177

Arroyave, F., Montaño, D., & Lizcano, F. (2020). Diabetes Mellitus Is a Chronic Disease that Can Benefit from Therapy with Induced Pluripotent Stem Cells. *Int J Mol Sci*, *21*(22). https://doi.org/10.3390/ijms21228685

Arvanitakis, Z., Tatavarthy, M., & Bennett, D. A. (2020). The Relation of Diabetes to Memory Function. *Curr Neurol Neurosci Rep*, *20*(12), 64. https://doi.org/10.1007/s11910-020-01085-9

Avilés-Santa, M. L., Monroig-Rivera, A., Soto-Soto, A., & Lindberg, N. M. (2020). Current State of Diabetes Mellitus Prevalence, Awareness, Treatment, and Control in Latin America: Challenges and Innovative Solutions to Improve Health Outcomes Across the Continent. *Curr Diab Rep*, *20*(11), 62. https://doi.org/10.1007/s11892-020-01341-9

Bathina, S., & Das, U. N. (2018). Dysregulation of PI3K-Akt-mTOR pathway in brain of streptozotocin-induced type 2 diabetes mellitus in Wistar rats. *Lipids in Health and Disease*, *17*(1), 168. https://doi.org/10.1186/s12944-018-0809-2

Bogdanov, P., Simó-Servat, O., Sampedro, J., Solà-Adell, C., Garcia-Ramírez, M., Ramos, H., Guerrero, M., Suñé-Negre, J. M., Ticó, J. R., Montoro, B., Durán, V., Arias, L., Hernández, C., & Simó, R. (2018). Topical Administration of Bosentan Prevents Retinal Neurodegeneration in Experimental Diabetes. *Int J Mol Sci*, *19*(11). https://doi.org/10.3390/ijms19113578

Cryer, M. J., Horani, T., & DiPette, D. J. (2016). Diabetes and Hypertension: A Comparative Review of Current Guidelines. *J Clin Hypertens (Greenwich)*, *18*(2), 95-100. https://doi.org/10.1111/jch.12638

Ighodaro, O. M., Adeosun, A. M., & Akinloye, O. A. (2017). Alloxan-induced diabetes, a common model for evaluating the glycemic-control potential of therapeutic compounds and plants extracts in experimental studies. *Medicina (Kaunas)*, *53*(6), 365-374. https://doi.org/10.1016/j.medici.2018.02.001

Karam, B. S., Chavez-Moreno, A., Koh, W., Akar, J. G., & Akar, F. G. (2017). Oxidative stress and inflammation as central mediators of atrial fibrillation in obesity and diabetes. *Cardiovasc Diabetol*, *16*(1), 120. https://doi.org/10.1186/s12933-017-0604-9

Nakhate, K. T., Yedke, S. U., Bharne, A. P., Subhedar, N. K., & Kokare, D. M. (2016). Evidence for the involvement of neuropeptide Y in the antidepressant effect of imipramine in type 2 diabetes. *Brain Res*, *1646*, 1-11. https://doi.org/10.1016/j.brainres.2016.05.035

Pascua-Maestro, R., Corraliza-Gomez, M., Diez-Hermano, S., Perez-Segurado, C., Ganfornina, M. D., & Sanchez, D. (2018). The MTT-formazan assay: Complementary technical approaches and in vivo validation in Drosophila larvae. *Acta Histochem*, *120*(3), 179-186. https://doi.org/10.1016/j.acthis.2018.01.006

Redl, K., Breu, W., Davis, B., & Bauer, R. (1994). Anti-inflammatory active polyacetylenes from Bidens campylotheca. *Planta Medica*, *60*(58-62).

Sarma Kataki, M., Murugamani, V., Rajkumari, A., Singh Mehra, P., Awasthi, D., & Shankar Yadav, R. (2012). Antioxidant, hepatoprotective, and anthelmintic activities of methanol extract of Urtica dioica L. leaves. *Pharmaceutical Crops*, *3*(1).

Seelinger, G., Merfort, I., & Schempp, C. M. (2008). Anti-oxidant, anti-inflammatory and anti-allergic activities of luteolin. *Molecules*, *13*(10), 2628-2651. https://doi.org/10.3390/molecules13102628

Tadros, M. I., & Fahmy, R. H. (2014). Controlled-release triple anti-inflammatory therapy based on novel gastroretentive sponges: characterization and magnetic resonance imaging in healthy volunteers. *Int J Pharm*, *472*(1-2), 27-39. https://doi.org/10.1016/j.ijpharm.2014.06.013

Wong, C. Y., Al-Salami, H., & Dass, C. R. (2017). Potential of insulin nanoparticle formulations for oral delivery and diabetes treatment. *J Control Release*, *264*, 247-275. https://doi.org/10.1016/j.jconrel.2017.09.003

Xing, H., Wang, H., Wu, B., & Zhang, X. (2017). Lipid nanoparticles for the delivery of active natural medicines. *Curr Pharm Des*. https://doi.org/10.2174/1381612824666171128105853

Zhao, Y., Chang, Y. X., Hu, X., Liu, C. Y., Quan, L. H., & Liao, Y. H. (2017). Solid lipid nanoparticles for sustained pulmonary delivery of Yuxingcao essential oil: Preparation, characterization and in vivo evaluation. *Int J Pharm*, *516*(1-2), 364-371. https://doi.org/10.1016/j.ijpharm.2016.11.046

Zoubari, G., Staufenbiel, S., Volz, P., Alexiev, U., & Bodmeier, R. (2017). Effect of drug solubility and lipid carrier on drug release from lipid nanoparticles for dermal delivery. *Eur J Pharm Biopharm*, *110*, 39-46. https://doi.org/10.1016/j.ejpb.2016.10.021